Available online at www.sciencedirect.com
ScienceDirect
Icarus 194 (2008) 800–810
ICARUS
www.elsevier.com/locate/icarus

On oligarchic growth of planets in protoplanetary disks

Adrián Brunini [a,b,*,1], Omar G. Benvenuto [a,b,2]

[a] *Facultad de Ciencias Astronómicas y Geofísicas, Universidad Nacional de La Plata, Paseo del Bosque s/n, 1900 La Plata, Argentina*
[b] *Instituto de Astrofísica de La Plata (IALP), Paseo del Bosque s/n, 1900 La Plata, Argentina*

Received 12 March 2007; revised 25 October 2007

Available online 14 December 2007

Abstract

In this paper we present a new semianalytical model of oligarchic growth of planets considering a distribution of planetesimal sizes, fragmentation of planetesimals in mutual collisions, sublimation of ices through the snow line, random velocities out of equilibrium and merging of planetary embryos. We show that the presence of several planetary embryos growing simultaneously at different locations in the protoplanetary disk affects the whole accretion history, specially for the innermost planets. The results presented here clearly indicate the relevance of considering a distribution of planetesimal sizes. Fragmentation occurring during planetesimal–planetesimal collisions represent only a marginal effect in shaping the surface density of solid material in the protoplanetary disc.

Keywords: Accretion; Planetary formation; Planetesimals

1. Introduction

The core instability model (Mizuno, 1980; Bodenheimer and Pollack, 1986; Pollack et al., 1996; Benvenuto and Brunini, 2005; Fortier et al., 2007) is at present the paradigm of giant planet formation. In the frame of this model, a planetary embryo first grows by accretion of solid planetesimals. If it is able to reach some Earth masses while the surrounding primordial gas is still present in the protoplanetary nebula, the nebular gas starts to be accreted onto the solid core in a runaway fashion. Although the cause of the termination of the accretion of gas is not yet well understood, the whole process ends up with a giant planet formed by a solid core plus a dense gaseous envelope. The core instability process has been studied either by analytical methods or numerical ones, with an increasing degree of details during the last three decades (Mizuno, 1980; Stevenson, 1982; Bodenheimer and Pollack, 1986; Pollack et al., 1996). In this paper we will focus our attention to some aspects of the accretion process of the solid cores of giant planets.

In a protoplanetary disk, the first mode of solid accretion is runaway growth (Greenberg, 1980), where the largest bodies grow much faster than the smaller ones. In this regime, the self interaction between planetesimals dominates the dynamical evolution of the disk. The relative velocities are slow enough so the gravitational cross section of the big planetesimals are the bigger ones. However, at later times, the largest objects become massive enough such that their influence dominates the dynamical evolution of the surrounding planetesimals, increasing the relative velocities. Then, the accretion process of these embryos switches to a slower regime, where the growth rate of adjacent protoplanets tends to unity over time. This mode of accretion was called "oligarchic growth" (Kokubo and Ida, 1998, 2000, 2002). The transition from runaway to oligarchic growth is produced very early, when the mass of the protoplanets are still orders of magnitude smaller than one Earth mass (Ida and Makino, 1993; Thommes et al., 2003). Therefore, since very early times, the relevant regime for modeling the accretion of solid cores of giant planets is the oligarchic growth.

Several models of oligarchic growth of solid cores have been presented in the last years (Thommes et al., 2003;

* Corresponding author at: Facultad de Ciencias Astronómicas y Geofísicas, Universidad Nacional de La Plata, Paseo del Bosque s/n, 1900 La Plata, Argentina.
E-mail address: abrunini@fcaglp.unlp.edu.ar (A. Brunini).
[1] Member of the Carrera del Investigador Científico, Consejo Nacional de Investigaciones Científicas y Técnicas (CONICET).
[2] Member of the Carrera del Investigador Científico, Comision de investigaciones Científicas de la Provincia de Buenos Aires (CIC).

0019-1035/$ – see front matter
doi:10.1016/j.icarus.2007.11.013

Chambers, 2006) each one including different physical phenomena. Thommes et al. (2003) developed a model of oligarchic growth where the random velocity of the planetesimals is assumed to be in equilibrium. They also considered a single-sized population of planetesimals, including the effect of planetesimal drift through the disc due to gas drag. Thommes et al. (2003) found that the largest final protoplanet masses are smaller than those given by the isolation mass. They conclude that the oligarchic growth model appears to provide an upper limit for the efficiency of giant planet formation. Chambers's model (Chambers, 2006) explicitly computes the evolution of planetesimal eccentricities and inclinations, and includes also other effects such as planetesimal fragmentation, the enhancement of embryo capture cross section due to atmospheres and embryo–embryo collisions. He shows that it is possible to form 10 Earth-mass cores at 5 AU within plausible values of the model parameters. These models coincides in that the size of the planetesimals plays an important role in the accretion of planets.

Here we will present a new semianalitycal model of oligarchic growth which includes a realistic size distribution of planetesimals, fragmentation through planetesimal mutual collisions, sublimation of ices and embryo–embryo collisions in a rather realistic way.

The present paper is organized as follows: in Section 2 we describe the main ingredients of our model including the way we handled the process of accretion, the description we assumed for the velocities of planetesimals outside equilibrium conditions, the treatment of the planetesimal drift due to gas drag, the effect of the sublimation of ices through the snow line. We also describe in this section the distribution of sizes of planetesimals we have considered, presenting the way we handled fragmentation. In Section 3 we detail the initial conditions for our nominal models. In Section 4 we present the results of our numerical simulations. Finally, in Section 5 we discuss the relevance of the presented results and make some concluding remarks.

2. The model

2.1. Accretion onto the cores

The core accretion process is well described by the "particle in a box" approximation (Inaba et al., 2001)

$$\frac{\mathrm{d}M_P}{\mathrm{d}t} = \frac{2\pi\,\Sigma(R_P)R_H^2}{P}P_{\mathrm{coll}}, \tag{1}$$

where M_P is the mass of the planet $\Sigma(R_P)$ is the surface density of solids of the disk at the location of the planet, $R_H = R_P(M_P/3M_*)^{1/3}$ is the Hill radius of the planet, R_P is the radius of the orbit of the planet, M_* is the mass of the central star of the system, P is the orbital period, and the collision probability P_{coll} takes several forms depending on the planetesimals' random velocities (Chambers, 2006). In the high, medium and low velocity regimes, P_{coll} is given by

$$P_{\mathrm{high}} = \frac{(R+r)^2}{2\pi R_H^2}\left[I_F(\beta) + \frac{6R_H I_G(\beta)}{(R+r)\hat{e}^2}\right], \tag{2}$$

$$P_{\mathrm{med}} = \frac{(R+r)^2}{4\pi R_H^2\hat{i}}\left[17.3 + \frac{232R_H}{(R+r)}\right], \tag{3}$$

$$P_{\mathrm{low}} = 11.3\left(\frac{R+r}{R_H^2}\right)^{1/2}, \tag{4}$$

where R and r are the planet's and planetesimal's radius, respectively. $\hat{e}$ and $\hat{i}$ are the reduced eccentricity and inclination, given by $\hat{e} = eR_P/R_H$ and $\hat{i} = iR_P/R_H$, respectively, with $\beta = \hat{i}/\hat{e}$; e and i are the r.m.s. eccentricity and inclination of the planetesimals in the feeding zone. $I_F(\beta)$ and $I_G(\beta)$ are given in term of complete elliptic integrals, but in the domain $0 < \beta \leqslant 1$ they are well represented (within a 3% of error) by (Chambers, 2006)

$$I_F(\beta) = \frac{1 + 0.95925\beta + 0.77251\beta^2}{\beta(0.13142 + 0.12295\beta)},$$
$$I_G(\beta) = \frac{1 + 0.39960\beta}{\beta(0.0369 + 0.048333\beta + 0.006874\beta^2)}.$$

The high-velocity expressions are appropriate in case $\hat{e}, \hat{i} > 2$ while the low-velocity expressions should be used if $\hat{e}, \hat{i} < 0.2$. In any other case, the medium-velocity expressions have to be adopted.

Let us define the feeding zone as the ring around the protoplanet where planetesimals can be accreted. The width of the feeding zone is usually taken as b times the protoplanet's Hill radius, with $b = 10$ (Thommes et al., 2003). In order to properly account for the width of the feeding zone, we have generalized Eq. (1) by writing

$$\frac{\mathrm{d}M_P}{\mathrm{d}t} = \int_{\mathrm{FZ}} 2\pi\,\psi(a, R_H, R_P)\frac{2\pi\,\Sigma(a)R_H^2}{P}P_{\mathrm{coll}}a\,\mathrm{d}a, \tag{5}$$

where a is the distance from the central star. We have chosen a functional form of $\psi(a, R_H, R_P)$ imposing a normalization condition $\int_{\mathrm{FZ}} 2\pi\,\psi(a, R_H, R_P)a\,\mathrm{d}a = 1$ (FZ indicates that the integration extends over the feeding zone). In this paper we have employed

$$\psi(a, R_H, R_P) = \frac{1}{2\pi^{3/2}b}\exp\left[-\left(\frac{a - R_P}{bR_H}\right)^2\right]. \tag{6}$$

The planetesimal-core relative velocity v_{rel} may be described as

$$v_{\mathrm{rel}} = \sqrt{\frac{5}{8}e^2 + \frac{1}{2}i^2}v_k, \tag{7}$$

where v_k is the Keplerian velocity at the distance R_P. The relative velocity is governed by the gravitational stirring due to the protoplanets and the damping due to gas drag. The former can be modeled as (Ohtsuki et al., 2002)

$$\left(\frac{\mathrm{d}\langle e^2\rangle}{\mathrm{d}t}\right)_{\mathrm{stirr}} = \left(\frac{M_P}{3bM_*P}\right)P_{\mathrm{VS}},$$
$$\left(\frac{\mathrm{d}\langle i^2\rangle}{\mathrm{d}t}\right)_{\mathrm{stirr}} = \left(\frac{M_P}{3bM_*P}\right)Q_{\mathrm{VS}}, \tag{8}$$

where P_{VS}, Q_{VS} are given by

$$P_{VS} = \left[\frac{73\hat{e}^2}{10\Lambda^2}\right]\ln\left(1+\frac{10\Lambda^2}{\hat{e}^2}\right)+\left[\frac{72I_{PVS}(\beta)}{\pi\hat{e}\hat{i}}\right]\ln\left(1+\Lambda^2\right),$$
$$Q_{VS} = \left[\frac{4\hat{i}^2+0.2\hat{i}\hat{e}^3}{10\Lambda^2\hat{e}}\right]\ln\left(1+10\Lambda^2\hat{e}\right)+\left[\frac{72I_{QVS}(\beta)}{\pi\hat{e}\hat{i}}\right]\ln\left(1+\Lambda^2\right). \quad (9)$$

$\Lambda = \hat{i}(\hat{i}^2+\hat{e}^2)/12$; $I_{PVS}(\beta)$ and $I_{QVS}(\beta)$ are given by elliptic integrals that are well approximated by [Eqs. (21) of Chambers (2006)]

$$I_{PVS}(\beta) = \frac{\beta - 0.36251}{0.061547 + 0.16112\beta + 0.054473\beta^2},$$
$$I_{QVS}(\beta) = \frac{0.71946 - \beta}{0.21239 + 0.49764\beta + 0.14369\beta^2}.$$

However, this velocity drops substantially as we go farther from the protoplanet. Hasegawa and Nakazawa (1990) have shown that when the distance to the protoplanet is >3.5–4 Hill radius, the planet is no longer able to substantially excite the planetesimal relative velocities. Therefore, we have represented the eccentricity stirred by the protoplanet as

$$\left(\frac{d\langle e^2\rangle}{dt}\right)^{\text{eff}}_{\text{stirr}} = f(\Delta)\left(\frac{d\langle e^2\rangle}{dt}\right)_{\text{stirr}}, \quad (10)$$

where

$$f(\Delta) = \left(1+\left\|\frac{\Delta}{10R_H}\right\|^5\right)^{-1}, \quad (11)$$

where Δ is the distance to the protoplanet. We adopted the same prescription for the orbital inclination. $f(\Delta)$ guarantees that the velocity profile along the planetesimal disk is smooth enough. This is an important question in order to solve adequately the redistribution of solids through the planetesimal disc due to gas drag (see the next subsection). The fifth power in $f(\Delta)$ is rather arbitrary, and it was adopted to make the effects due to the presence of a planetary object mainly restricted to its feeding zone. It is worth noting that we have ran all our numerical simulations using different powers finding no appreciable differences in the final results.

The drag caused by the gaseous component of the protoplanetary disk damps out the orbital eccentricities and inclinations of the planetesimals at a rate (Adachi et al., 1976)

$$\left(\frac{de}{dt}\right)^{\text{gas}} = \frac{\pi e r^2 C_D \rho_{\text{gas}} v_k}{2m}\left(\eta^2+v_{\text{rel}}^2\right),$$
$$\left(\frac{di}{dt}\right)^{\text{gas}} = \frac{\pi i r^2 C_D \rho_{\text{gas}} v_k}{4m}\left(\eta^2+v_{\text{rel}}^2\right), \quad (12)$$

where r is the radius of the planetesimals, C_D a dimensionless drag coefficient (of order 1 for spherical planetesimals), m the planetesimal mass and ρ_{gas} is the density of the nebular gas at the distance a from the central star. η is the fractional difference between the gas velocity and the local Keplerian velocity, arising from the partial pressure support of the gas disk, and it is given by

$$\eta = \frac{v_k - v_{\text{gas}}}{v_k} = \frac{\pi}{16}(\alpha+\beta)\left(\frac{c_s}{v_k}\right)^2, \quad (13)$$

where β is the temperature profile index of the nebula ($T(a) \propto a^{-\beta}$) and c_s the sound speed. We assume that the disk scale height is $z = 0.05a^{5/4}$, and therefore $c_s/v_k = 0.05a^{1/4}$. Drag is strongly dependent on the planetesimal sizes.

Some previous models of oligarchic growth assumed that planetesimals attain an equilibrium relative velocity. Thommes et al. (2003) proposed that this assumption is valid as long as the embryos reach masses larger than 10^{-2}–10^{-1} $M_\oplus$. Previous to this condition, the equilibrium cannot be attained, because the accretion timescale is shorter than the timescale to reach the equilibrium. Nevertheless, it is not clear that an equilibrium condition is ever achieved, specially for small planetesimals (Chambers, 2006). Therefore, for each planetesimal population (see below), at each distance from the central star, we integrate Eqs. (10) and (12) by a semi-implicit Euler integrator (Gear, 1971). The employment of a semi-implicit method provides numerical stability either near as well as far from equilibrium conditions.

For this study we used a surface density of solids based in the minimum mass solar nebula model (hereafter MMSN) of Hayashi et al. (1985):

$$\Sigma(a) = 7.1\left(\frac{a}{1\text{ AU}}\right)^{-3/2}\text{g cm}^{-2}, \quad a < 2.7\text{ AU},$$
$$\Sigma(a) = 30\left(\frac{a}{1\text{ AU}}\right)^{-3/2}\text{g cm}^{-2}, \quad a > 2.7\text{ AU}. \quad (14)$$

The discontinuity at 2.7 AU is due to the condensation of volatiles (the "snow line") that in the present Solar System occurs at this distance from the Sun. Because of numerical reasons we follow Thommes et al. (2003) spreading the "snow line" in a region of about 1 AU with a smooth function:

$$\Sigma(a) = \left\{7.1+(30-7.1)\left[\frac{1}{2}\tanh\left(\frac{a-2.7}{0.5}\right)+\frac{1}{2}\right]\right\}\times\left(\frac{a}{1\text{ AU}}\right)^{-3/2}\text{g cm}^{-2}. \quad (15)$$

For the gas density profile we used the mid-plane value of the MMSN model which is given by

$$\rho_{\text{gas}} = 1.4\times10^{-9}\left(\frac{a}{1\text{ AU}}\right)^{-\alpha}\text{g cm}^{-3}, \quad (16)$$

with $\alpha = 11/4$.

In this paper we assume that the gas of the protoplanetary nebula uniformly decays throughout all the disk with an exponential decay rate with characteristic timescale of 10 Myr. This is a simplification to the actual situation in which the gas density of the disk should be computed by solving the equation of angular momentum conservation (see, e.g., Pringle, 1981). We shall account for this effect, beyond the scope of the present work, in a further paper.

2.2. Planetesimal drift by gas drag

Planetesimals are subject to gas drag, which causes a radial mobility of them and affects the distribution of solids in the disk. As it was shown by Thommes et al. (2003) and Chambers

(2006), this effect has a strong influence on the timescales of accretion, and also on the final masses that planets achieve at different locations in the protoplanetary disk. Planetesimal drift is described by (Adachi et al., 1976)

$$\frac{\mathrm{d}a}{\mathrm{d}t} = -\frac{2a}{T_{\mathrm{drag}}}\left(\eta^2 + \frac{5}{8}e^2 + \frac{1}{2}i^2\right)^{1/2} \times \left[\eta + \left(\frac{5}{16} + \frac{\alpha}{4}\right)e^2 + \frac{1}{4}i^2\right], \quad (17)$$

where

$$T_{\mathrm{drag}} = \frac{8\rho r}{3C_D\rho_{\mathrm{gas}}v_k}, \quad (18)$$

where ρ is the planetesimal density.

The planetesimal disk evolution obeys the continuity equation. If we integrate in the z-direction and assume axial symmetry, it can be written as

$$\frac{\partial\Sigma}{\partial t} - \frac{1}{a}\frac{\partial}{\partial a}\left(a\frac{\mathrm{d}a}{\mathrm{d}t}\Sigma\right) = F(a), \quad (19)$$

where $F(a)$ represents all the sink terms that subtract material from the disc (see below for further details).

One of the sink terms is due to accretion onto one planet, and it is given by

$$F_{\mathrm{acc}}(a) = -\frac{\mathrm{d}M_P}{2\pi a\,\mathrm{d}a\,\mathrm{d}t} = -\psi(a, R_H, R_P)\frac{2\pi\Sigma R_H^2}{P}P_{\mathrm{coll}}. \quad (20)$$

Of course, in the case that more than one planet is present we should add the contributions to $F_{\mathrm{acc}}(a)$.

This partial differential equation was numerically solved using a fully implicit method. Because of the characteristics of the problem we are interested in here, we found it very adequate to employ a logarithmic evenly spaced grid. The number of zones has been variable. Initially we set a very fine grid of 8000 mesh points. This is important in order to allow for the presence of some points inside the feeding zones of each protoplanet. Notice that, initially, the planetary masses are very tiny ($\approx 1\times10^{-3}\ M_\oplus$) and so, the corresponding feeding zones.

2.3. Sublimation of ices

75% of the material beyond the snow line is composed of volatile ices. When ice rich planetesimals coming from the outer part of the disk reach the snow line, they sublimate like cometary nuclei (it is worth noting that some comets become dust mantled and dormant, and may retain a significant fraction of their volatiles in their deep interior, but this possibility was not taken into account in our model). The sublimation process is indeed very complex, and a detailed model is out of the scope of the present paper. We treat this effect in a very simplified way, by including a sink term F_{ice} with appreciable values on a finite zone, as done for the shape of the initial density profile [Eq. (15)]. The adopted expression is of the form

$$F_{\mathrm{ice}}(a) = -\frac{0.75\Sigma(a)}{\Delta_{\mathrm{ice}}\sqrt{\pi}}v_p\exp\left[-\left(\frac{a-R_{\mathrm{ice}}}{\Delta_{\mathrm{ice}}}\right)^2\right], \quad (21)$$

where v_p is the radial velocity of the considered planetesimal of a given radius. This prescription guarantees the evaporation of the 75% of the planetesimal material on an annulus of $\approx\Delta_{\mathrm{ice}}/2$, because this sink term was applied only if $a \leqslant R_{\mathrm{ice}}$ that we set as $R_{\mathrm{ice}} = 2.7$ AU. For the parameter Δ_{ice} a brief discussion is in order. The sublimation lifetime depends on the planetesimal radius. For a planetesimal of 1 km, composed of water ice, Fernández (2005) estimate a lifetime of ∼1500 orbital revolutions at 2 AU (a value computed for the conditions in the present Solar System), being the lifetime proportional to the planetesimal radius. This lifetime is much shorter than the characteristic drift timescale in the disk due to gas drag. At 2 AU, planetesimals spend

$$T_{\mathrm{drag}} \sim 2.7\times10^7\left[\frac{r}{1\ \mathrm{km}}\right]\ \mathrm{yr}, \quad (22)$$

to travel 1 AU. However, as it will be seen in Section 4, the maximum planetesimal drift velocity, which is reached around the ice line, range between $\sim300\ \mathrm{cm\,s^{-1}}$ for the smallest planetesimals to $\sim30\ \mathrm{cm\,s^{-1}}$ for the largest ones, because inward drift becomes faster when bodies move on eccentric orbits, which is the case when nearby cores become large. Therefore, the characteristic drift timescale may be much shorter than the one computed by Eq. (22).

Assuming that the mass sublimation rate is proportional to the surface area of the planetesimals, it results that the timescale of sublimation of a planetesimal of radius r could be modeled as

$$T_{\mathrm{sub}} = T_0\left(\frac{r}{1\ \mathrm{km}}\right), \quad (23)$$

where T_0 is the timescale of sublimation of an object of $r =$ 1 km, that we adopt as $T_0 = 5000$ yr. The distance these planetesimals travel during T_{sub} is

$$\mathrm{Dist} = T_{\mathrm{sub}}v_p. \quad (24)$$

Therefore, we adopt this distance as Δ_{ice} in Eq. (21). v_p is not only a function of the planetesimal radius but also of the distance to the central star. Nevertheless we adopt a fixed value for v_p equal to its value at the snow line. It is worth noting that for $r = 0.1$ km, Δ_{ice} could reach at most a value of ∼0.3 AU. Therefore the sublimation of the smallest objects takes place on a narrow region around the ice line. On the contrary, for 100 km planetesimals Δ_{ice} may be very large (several AU). This implies that these planetesimals are almost not sublimated at all. Nevertheless, half of the total mass in our distribution is in objects with $r \leqslant 0.2$ km, and therefore the snow line will be always present in our simulations.

2.4. Size distribution of planetesimals

In previous studies of this same kind (Thommes et al., 2003) an uniform size distribution, or at most a bimodal size distribution composed of planetesimals and fragments, was adopted. As we have done in the previous sections, the effect of the planetesimal size was addressed by making several independent

simulations using different planetesimal sizes. Small planetesimals makes accretion much faster, specially in the outer regions beyond the snow-line. This is indeed a crucial point for the core instability model, because the accretion of gas is only possible before its complete dispersal from the nebula. In view of these questions, we have generalized our program in order to deal with a spectrum of planetesimal sizes. To do this we have divided the population of planetesimals in 31 mass bins, from 1 m to ∼100 km (each bin has objects with twice the mass of the ones in the previous bin). We adopted a cumulative power law mass distribution of planetesimals of the form $\mathrm{d}N/\mathrm{d}m \propto m^{\alpha}$ with $\alpha = -2.5$, consistent with the results of Kokubo and Ida (1998, 2000) for the spectrum of masses of a population that has relaxed to isolated runaway bodies. Each size has its own velocity evolution. Since the total mass is $\int nm\,\mathrm{d}m \propto m^{\alpha+2}$, most of the disk mass is contained in the small bodies.

We evolved a generalized version of Eq. (5) to allow for the presence of a distribution of planetesimal sizes

$$\frac{\mathrm{d}M_P}{\mathrm{d}t} = \int_{\mathrm{dist}} \mathrm{d}m \int_{FZ} 2\pi\psi(a, R_H, R_P) \times \frac{2\pi\Sigma(a,m)R_H^2}{P} P_{\mathrm{coll}}(a,m)a\,\mathrm{d}a, \tag{25}$$

where dist stands for the integration over the distribution of sizes of planetesimals. Here we have included explicitly the dependence of quantities upon the planetesimal mass. For details on how we performed the integral over the distribution of sizes, see Appendix A.

When a distribution of planetesimal sizes is present, the continuity equation [Eq. (19)] has to be solved for each size simultaneously. It is important to remark that, fortunately, the sink term due to accretion [see Eq. (20)] is diagonal, in the sense that we are able to compute the migration of each size of planetesimals *separately*. This were not the case, we would have to solve for all the sizes and grid positions simultaneously. This would be much more time consuming. The sink term due to ices [Eq. (21)], is also diagonal.

2.5. Fragmentation

We have also included, in a rather simplified way, the effect of fragmentation through collisions. Collisional activity generates small fragments that populates the smallest bins and de-populate the largest ones. In addition, in absence of migration due to gas drag, small fragments are more efficiently accreted by protoplanets (Wetherill and Stewart, 1993; Chambers, 2006), because they are quickly driven to circular orbits by gas drag, enhancing the gravitational cross section of the protoplanets respect to these small particles in a very substantial way (Chambers, 2006).

The impact relative velocity V and the shattering impact specific energy Q_S are two fundamental quantities determining, for a given body, the outcome of the collision. Q_S is the amount of energy per unit target mass needed to catastrophically fragment a body, such that the largest resulting fragment has half the mass of the original target, regardless of re accumulation of fragments. Benz and Asphaug (1999) have shown that for small bodies, with diameters <1 km, the material properties control the impact strength in such a way that it decreases with increasing size. On another hand, for diameters >1 km, gravity dominates the impact strength which increases with increasing size. Benz and Asphaug (1999) obtained an empirical expression for $Q_S(r)$, averaged over different impact orientations:

$$Q_S(r) = 3.5\times 10^7\left(\frac{r}{1\ \mathrm{cm}}\right)^{-0.38} + 1.36\rho\left(\frac{r}{1\ \mathrm{cm}}\right)^{1.36}\ [\mathrm{erg/g}]. \tag{26}$$

The relative kinetic energy in a collision between two bodies of masses m_l and m_j is given by

$$E_{\mathrm{rel}} = \frac{1}{2}\frac{m_l m_j}{m_l + m_j}V^2. \tag{27}$$

According to these definitions and assuming that the energy is equi-partitioned between the two colliding bodies, for body k fragmentation occurs if $E_{\mathrm{rel}} \geqslant 2Q_S(r_l)m_l$ (a similar expression holds for j). We assume that in this case all the mass m_l is converted in collisional fragments, whereas if $E_{\mathrm{rel}} < 2Q_S(r_l)m_l$, only a fraction $E_{\mathrm{rel}}/2Q_S(r_l)m_l$ of the mass is converted in fragments. The relative velocity between l and j is computed as

$$V = \sqrt{v_l^2 + v_j^2}, \tag{28}$$

where v_l and v_j are the planet–planetesimal relative velocities of each population, given by Eq. (7). We assume that the planets are on circular orbits. The number of collisions that planetesimals of radius r_l receives in time Δt by planetesimals of radius r_j is given by

$$N_{l,j} = \frac{\Sigma_l}{m_l 2h_l}\frac{\Sigma_j}{m_j 2h_j}\pi(r_l + r_j)^2 V\,\Delta t, \tag{29}$$

where Σ_l is the surface density of planetesimals of radius r_l at the distance a and $h_l \sim a i_l$ is their corresponding disk scale height. In this expression we have considered gravitational focusing that could be important when the smallest planetesimals, which have probably the smallest relative velocity, impact onto the largest one, which have the largest escape velocity. The total number of impacts is therefore $N_l = \sum_j N_{l,j}$. The mass of the disc in planetesimals of mass m_l in the zone is reduced by the amount $-m_l N_l f(E_{\mathrm{rel}})$ being

$$f(E_{\mathrm{rel}}) = E_{\mathrm{rel}}/2Q_S(l) \quad \text{if } E_{\mathrm{rel}} < 2Q_{S,l}m_l,$$
$$f(E_{\mathrm{rel}}) = 1 \quad \text{otherwise.} \tag{30}$$

Correspondingly, the surface density Σ_l is reduced by the quantity

$$\Delta\Sigma_l = -\frac{m_l N_l f(E_{\mathrm{rel}})}{2\pi a\,\Delta a}, \tag{31}$$

where Δa is the width of the zone. The mass loss from planetesimals of mass m_l, in the zone a is assumed to be redistributed in the form of fragments having a cumulative power low mass distribution of the form $N(>m) = m^{\beta}$ with $\beta = -11/6$

(Dohnanyi, 1969). Therefore we redistribute this mass through the mass bins l such that $m_l < m_l$, with this distribution law.

Regarding the way we handled fragmentation, we evolved one time step and then considered the effect of fragmentation, not including any sink term in the continuity equation (19). We did so because fragmentation is essentially an off-diagonal contribution. Then, our algorithm for solving the continuity equation may be regarded, in this sense, as semi-implicit.

In this model, we have not allowed for accretion or reaccumulation of fragments.

3. Initial conditions

In a nascent planetary system, protoplanet–protoplanet gravitational interaction tends to increase their orbital eccentricities and inclinations and expand their orbital separation. Dynamical friction from planetesimals damps out the eccentricities and the inclinations of the protoplanets in such a way that they expand their orbital separation, but always keeping nearly circular and coplanar orbits.

There is a typical orbital separation realized in the oligarchic growth stage. Kokubo and Ida (1998) found that the typical orbital separation of protoplanets is $\Delta a \sim \gamma \hat{R}_H$, where $\hat{R}_H$ is the mutual Hill's radius given by

$$\hat{R}_H = \left(\frac{(M_P)_1 + (M_P)_2}{3M_*} \right)^{1/3} \frac{(R_P)_1 + (R_P)_2}{2}. \tag{32}$$

In all our simulations we use $\gamma = 10$.

Ida and Makino (1993) derived the condition for the onset of the runaway growth stage, where protoplanet–planetesimal scattering dominates over planetesimal–planetesimal scattering in determining the evolution of the random velocities in the planetesimal disc. It is given by

$$2\Sigma_M M_P \sim \Sigma m, \tag{33}$$

where m is the effective planetesimal mass and Σ_M is the effective surface density of protoplanets in the planetesimal disc at the planet location. It is given by

$$\Sigma_M = \frac{M_P}{2\pi a \gamma \hat{R}_H}. \tag{34}$$

In the simulations presented in this paper, Eqs. (32) and (33) are solved to give the initial mass and location of the protoplanets for a given disc. Nevertheless, using the effective planetesimal mass m computed with the used distribution of planetesimal sizes, we obtain a too large number of initial protoplanets, making the numerical simulations impracticable. Thus we decided to set effective planetesimal mass for the first protoplanet $m = 1 \times 10^{23}$ g ($r \sim 200$ km). The first planet was placed at 0.5 AU and the last one at ≈20 AU. In this way we have generated 326, 262, 229, and 207 initial planets for the cases of 1, 3, 6, and 10 MMSN, respectively. These masses are larger than the ones given by Eq. (33), but we note that the initial accretion rate in most of the disk is so fast that they would have been reached very quickly, after few years of evolution, and we do not expect that our results could be sensitive to this assumption. As the protoplanets grow their mutual Hill's radii expands.

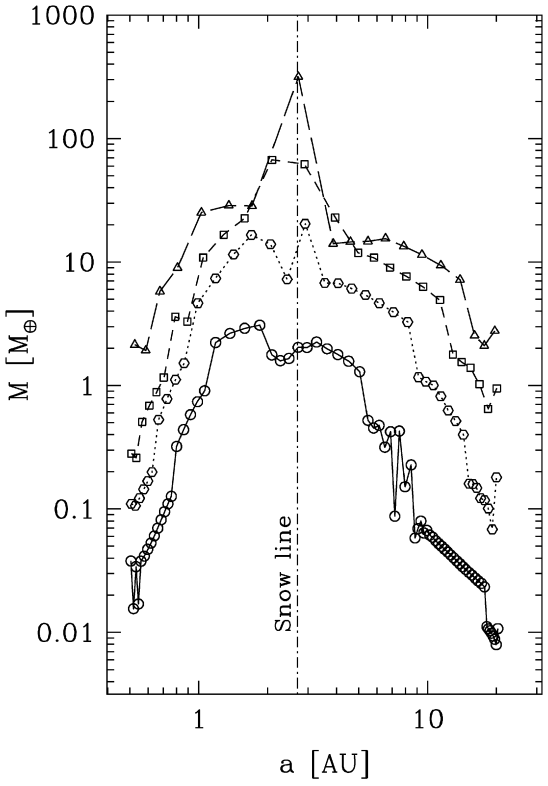

Fig. 1. The mass of the planets formed after 20 Myr as a function of the distance from the central star of the system. Circles connected with a solid line represent the mass and position of the planets corresponding to the case of a protoplanetary nebula of 1 MMSN. The results corresponding to the cases of 3, 6 and 10 MMSN are represented with hexagons (connected with a dotted line), squares (connected with a short dashed line), and triangles (connected with a long dashed line), respectively. The position of the snow line is shown for the sake of comparison.

When the distance between two adjacent protoplanets becomes less than $3.5R_H$, we allowed for the merging of them into one single object. The mergers were considered perfectly inelastic. Thus, the new protoplanet has the sum of the masses of the two progenitors and it is placed at a new distance to the central star by considering conservation of the orbital angular momentum, assuming circular orbits.

As initial conditions for the r.m.s. value of the planetesimal relative velocities, we used $e = 1 \times 10^{-4}$ and $i = e/2$.

4. Numerical results

In Fig. 1 we show the mass of the planets formed after 20 Myr as a function of the distance from the central star of the system for the four nebulae considered in this paper. In all explored cases, the most massive objects are formed in the neighborhood of the ice line. It is remarkable that, while the masses of the considered nebulae differ in an order of magnitude, the most massive planet formed in the 10 MMSN is ≈100 times larger than the corresponding to the 1 MMSN. We find that the mass of the planets is a strongly decreasing function at both sides of the position of the maximum. Also, there are noticeable boundary effects at the edge of the regions where we allowed for the presence of planets. Systematically, the out-

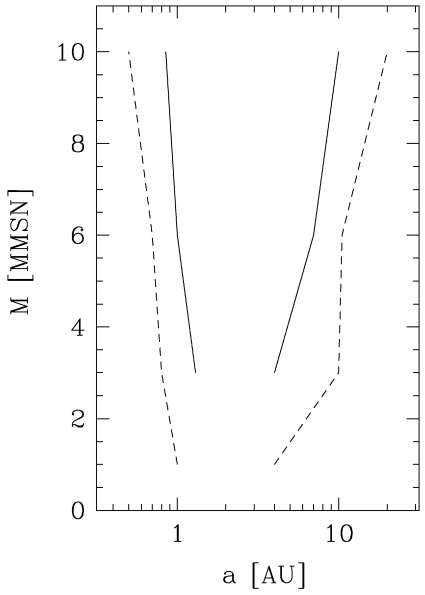

Fig. 2. The limits of the zone inside which planets of more than 1 $M_\oplus$ (long dashed lines) and 10 $M_\oplus$ are formed (solid lines) as a function of the mass of the nebula inside which they have grown. For the case of 1 MMSN no planet has reached 10 $M_\oplus$. The zone where objects more massive than 10 $M_\oplus$ can form represents the places where the mass of gas bounded to the planets should be relevant. There is where we should expect the occurrence of objects able to reach runaway gas accretion conditions.

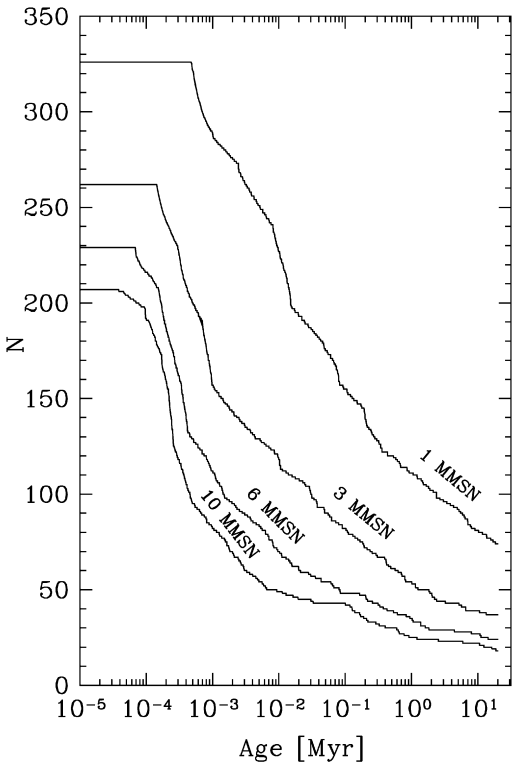

Fig. 3. The number of planets as a function of time for the four nebulae considered in this paper. We find that the number of objects is larger the lower is the mass of the nebula. This is due not only to the fact that objects are initially more numerous (see Section 4) but also because planets grow at lower rates, making it more difficult to fulfill the conditions for the occurrence of merging (notice that for the case of 1 MMSN planetary merging begins at ages ≈10 times larger as compared to the case of 10 MMSN). Also, we see that for the case of massive nebulae, the accretion is almost negligible after 20 Myr of evolution. This is not the case for the system corresponding to the 1 MMSN nebula.

ermost/innermost planet in all the simulations is more massive than its neighbors. This is because the neighbors have planets on both sides competing for the accretion of material.

In Fig. 2 we show the limits of the zone inside which planets of more than 1 $M_\oplus$ and 10 $M_\oplus$ are formed as a function of the mass of the nebula inside which they have grown. For the case of 1 MMSN no planet has reached 10 $M_\oplus$. It is worth noting that the gaseous envelope of the planets was ignored in this paper. In the case of planets with a solid core with a mass $\lesssim$10 $M_\oplus$, the amount of gas bounded to the core is small and we expect the description presented in this paper to be essentially correct. However, for the case of more massive cores, runaway gas accretion conditions may be reached, and the mass of the planet may be much larger than this core mass. The presence of a gas envelope has several consequences that should be analyzed. On the one hand, it increases the planet cross section as planetesimals are slow down by gas drag within the planet atmosphere (Brunini and Melita, 2002; Inaba and Ikoma, 2003). On the another hand, the mass of the atmosphere increases the feeding zone, affecting also the sequence of merging. These effects will be analyzed in a forthcoming paper. The zone where objects more massive than 10 $M_\oplus$ can form represents the places where the mass of gas bounded to the planets should be relevant. There is where we should expect the occurrence of objects able to reach runaway gas accretion conditions. Note that for plausible values of what we think was the mass of the solar nebula, the region where 10 $M_\oplus$ could form is rather compact, in concordance with some recent models of the formation of the outer solar system (Tsiganis et al., 2005).

In Fig. 3 we show the number of planets as a function of time for the four nebulae considered in this paper. The number of planets is larger, the smaller is the mass of the nebula. This is not only due to the fact that the objects are initially more numerous [because smaller planets are tightly spaced, see Eqs. (33) and (34)] but also because planets grow slowly in less massive nebulae, making it more difficult to fulfill the conditions for the occurrence of merging (notice that for the case of 1 MMSN planetary merging begins at ages ≈10 times larger as compared to the case of 10 MMSN). Also, we see that after 20 Myr of evolution, the planetary systems for the case of massive nebulae have reached nearly equilibrium conditions. This is not the case for the system corresponding to the 1 MMSN nebula, because the system is not completely depleted of solid material and, in addition, accretion is still possible, because the planets are not massive enough to excite high planetesimal random velocities and stop the accretion.

Fig. 4 depicts the mass of the most massive planet as a function of time for the four nebulae considered in this paper. Notice that at early ages most of the mass of the most massive object is gained by merging. However, the most important merging is the last one in which it approximately increases its mass by a factor of ≈2. For 1 MMSN, the largest planet has only ∼3 $M_\oplus$.

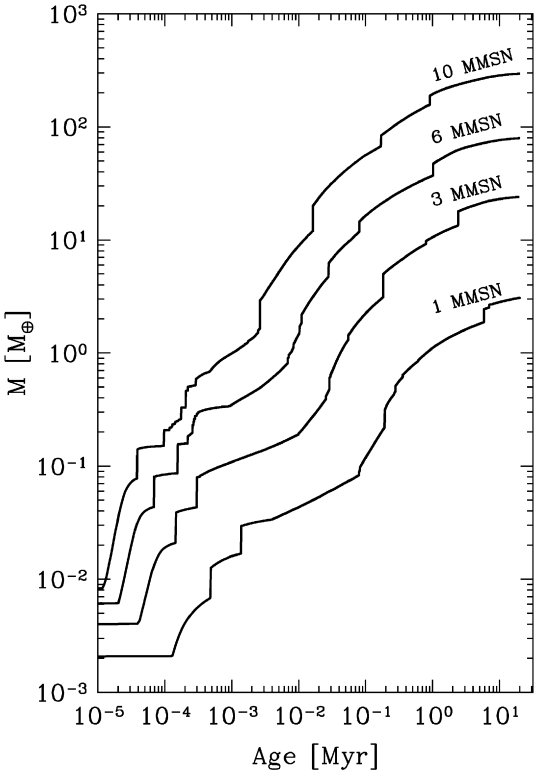

Fig. 4. The mass of the most massive planet as a function of time for the four nebulae considered in this paper. Notice that at early ages most of the mass of the most massive object is gained by merging. However, the most important merging is the last one in which it approximately increases its mass in ≈50%.

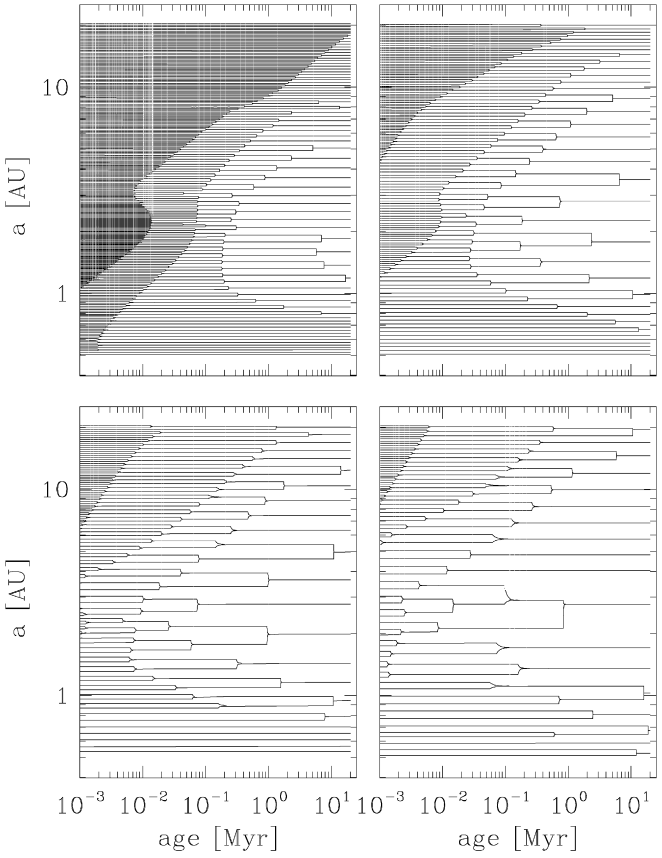

Fig. 5. The sequence of merging during the evolution of the planetary system evolving in 1 MMSN (upper left panel), 3 MMSN (upper right panel), 6 MMSN (lower left panel), and 10 MMSN (lower right panel) protoplanetary nebulae. Horizontal lines represent the position of a planet. Merging of two planets corresponds to the merging of two lines. From these plots we can visualize the sequences of merging over the entire nebulae evolution; e.g. for the case of 1 MMSN, merging occur initially at short distances from the central star. However, due to the planetesimal depletion of the inner nebula, planets cease to undergo a large growth and do not merge up to the end of our simulation. At distances from 1 to 5 AU, there is still some material available in the nebula, planets are still growing and are able to undergo supplementary mergers. Farther from the star, the planets reach lower masses and then merging are severely delayed. For more details, see the main text.

In Fig. 5 we show the sequence of merging during the evolution of the planetary system. From these plots we can visualize the sequences of merging over the entire nebulae evolution. For the case of 1 MMSN, merging occur initially at short distances from the central star and even are repeated previous to the occurrence at farther distances. However, due to the planetesimal depletion of the inner nebula, planets cease to undergo a large growth and do not merge up to the end of our simulation. At distances from 1 to 5 AU, there is still some material available in the nebula, planets are still growing and are able to undergo supplementary mergers. This region, around the snow line, is the most favorable for the emergence of large planets. Farther from the star, the planets reach low masses and then merging are severely delayed.

In Fig. 6 we show the density profile of the planetesimal disc corresponding to the case of 6 MMSN. We show this case because it contains all the physical phenomenology which is present in the four studied cases. Smaller planetesimals are quickly accreted at the inner part of the disc. As they represent most of the disc mass, a substantial accretion of planetesimals at later times is almost inhibited for the planets there located. At later times, planetesimal drift replenishes this zone with the smaller planetesimals (see Fig. 7). For the cases of planetesimals of 1, 10, and 100 km, neither accretion nor planetesimal drift are efficient. As consequence, there appears a local minimum in the density, located in the neighborhood of the ice line, where the larger planets are formed. The depletion of planetesimals of 1, 10, and 100 km, at the inner part of the disc and advanced ages is due mainly to drift, and not to accretion or fragmentation. For these sizes, with the exception perhaps of 1 km planetesimals, the conditions of replenishment are not reached after 20 Myr because the drift is much slower as compared to the case of the smallest considered objects of the distribution. As most of the mass is in the smaller objects, that are quickly removed from the system, there is a deficit of projectiles able to catastrophically disrupt the largest ones. As a consequence of this process, the production of fragments is not intense enough as to modify substantially the size distribution.

The planetesimal drift velocity as a function of the distance from the central star at different ages in the case of 6 MMSN is shown in Fig. 7. Here we show the extreme cases of 0.1 and 100 km planetesimals. The maximum in the velocity drift occurs in the neighborhood of the most massive planets, which are always located near the snow line. These planetesimals are

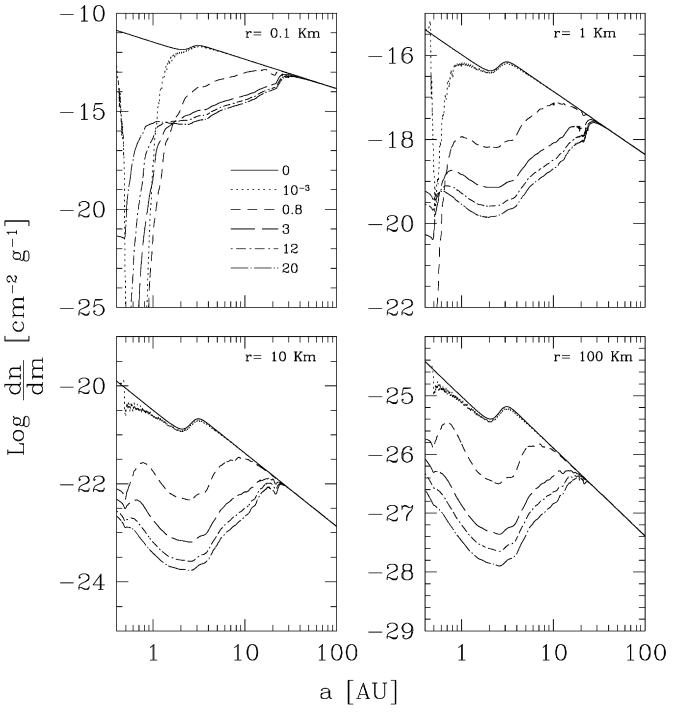

Fig. 6. The density profile of the planetesimal disc corresponding to the case of 6 MMSN. The smallest planetesimals (upper left panel) are quickly accreted at the inner part of the disc. As they represent most of the disc mass, a substantial accretion at later times is almost inhibited for the planets there located. At later times, planetesimal drift replenishes this zone. For the cases of planetesimals of 1, 10, and 100 km, neither accretion nor planetesimal drift are so efficient. As consequence, there appears a local minimum in the density, approximately located at the position of the ice line, where the larger planets are formed. The depletion of planetesimals of 1, 10, and 100 km, at the inner part of the disc and advanced ages is due mainly to drift. For these sizes, the conditions of replenishment are not reached because the drift is much slower as compared to the case of the smallest considered objects.

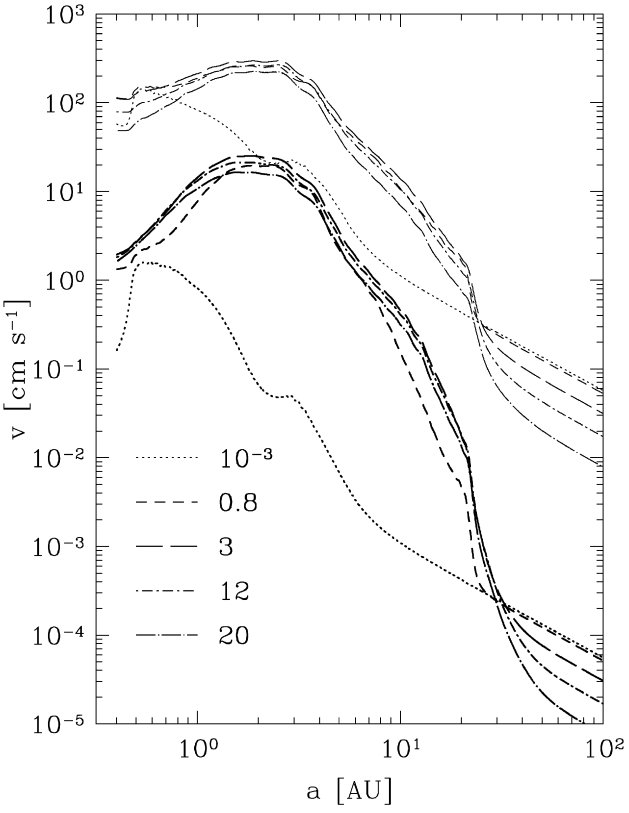

Fig. 7. The planetesimal drift velocity as a function of the distance from the central star at different ages in the case of 6 MMSN. Here we show the cases of 0.1 km (thin lines) and 100 km planetesimals (thick lines). The velocity drift maximum occurs in the zone of the disc where the most massive planets are located. This planetesimals are transferred to innermost regions where, as the velocity drift is much slower, they accumulate. This accumulation indeed occurs for the smallest planetesimals (see upper left panel of Fig. 6). However, for planetesimals of 100 km, this effect is not appreciable even at an age of 20 Myr (see lower right panel of Fig. 6), simply because in this case drift is much slower.

transferred to innermost regions where, as the velocity drift is much slower, they accumulate. This accumulation indeed occurs for the smallest planetesimals (see upper left panel of Fig. 6).

However, for planetesimals of 100 km, this effect is not appreciable even at an age of 20 Myr (see lower right panel of Fig. 6), simply because in this case drift is much slower.

In Fig. 8 we show the time evolution of the size distribution of planetesimals at different locations of the disc in the case of 6 MMSN. The differences in the timescales of radial drift and accretion for the different planetesimal populations, have remarkable consequences in the distribution of sizes at the innermost parts of the disc. Farther from the central star, the size distribution remains almost unaltered respect to the initial one.

The time evolution of the r.m.s. eccentricity and inclination of the 0.1 km planetesimals at different locations of the disc in the case of 6 MMSN is shown in Fig. 9. We observe that the system evolves from the initial condition very fast. This implies that the results are not sensitive to the initial e and i we adopted. This is consistent with the results reported by Chambers (2006). Equilibrium conditions in the dispersion dominated regime ($\beta \approx 0.5$) is partially reached only in the neighborhood of the most massive planet ($a \sim 2$ AU). In the rest of the disc, it is never reached. This fact illustrates the importance of adopting a time dependent evolution of e and i. As small planetesimals represent most of the mass in the planetesimal disc, results from models adopting equilibrium values should be taken with caution. The abrupt drop of e, i at ∼20–30 AU is due to the fact that we allowed for the presence of planets only for $a < 20$ AU. (We have repeated the simulations with planets up to 30 AU without noting any noticeable difference in the results.)

In order to asses the robustness of the results against some of the parameters of the model, we have repeated our runs with different sets of them. Firstly, we have performed runs with a characteristic timescale for the depletion of the nebular gas of 6 Myr. In this case the results were almost identical to the already previously shown. Another check we have performed is regarding to the initial mass of the protoplanets. We have carried out simulations with an initial planet mass reduced by a factor of 3 (a larger factor could imply a large number of planets that cannot be handled with our present computational resources). Although at very early ages the evolution of the planetary systems present some differences with our standard

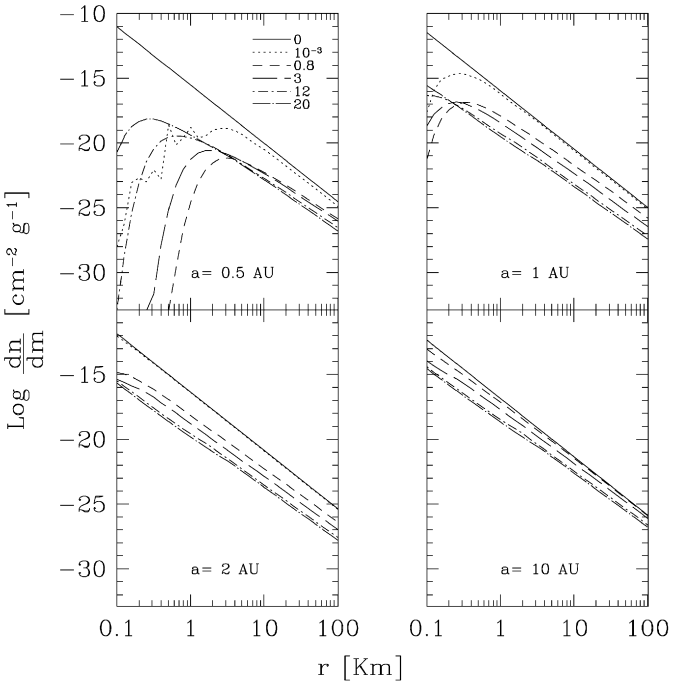

Fig. 8. The time evolution of the size distribution of planetesimals at different locations of the disc in the case of 6 MMSN. The differences in the timescales of radial drift and accretion for the different planetesimal populations, have a remarkable consequence in the distribution of sizes at inner locations. Farther from the central star, the size distribution remains almost unaltered respect to the initial one.

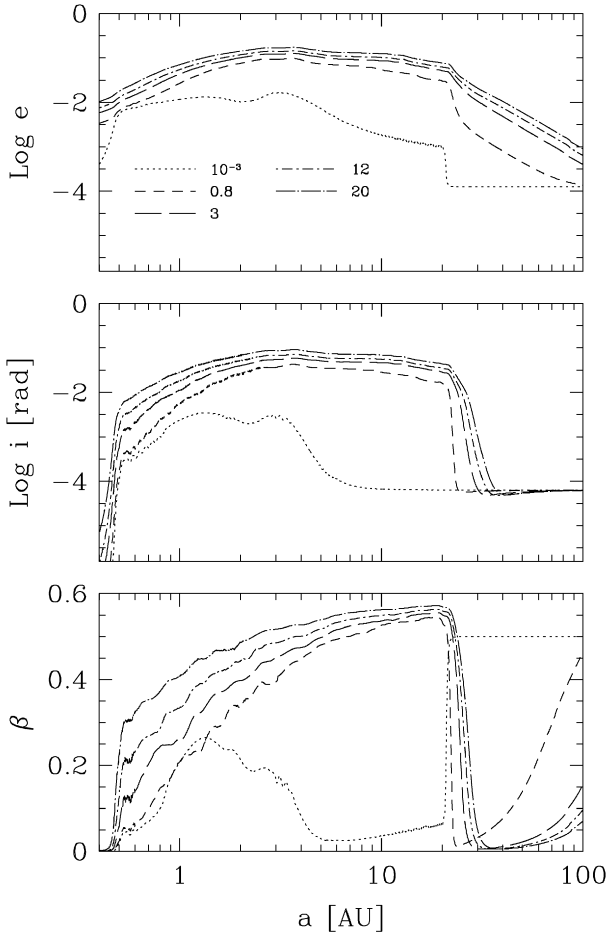

Fig. 9. The time evolution of the r.m.s. eccentricity and inclination of the 0.1 km planetesimals at different locations of the disc in the case of 6 MMSN. The bottom panel shows the parameter $\beta = i/e$. The dispersion dominated regime ($\beta \approx 0.5$) is only reached beyond the ice line. The abrupt drop of e, i at ∼20–30 AU is due to the fact that we allow for the presence of planets only for $a < 20$ AU.

models, they quickly attain the same behavior (even quantitatively). We conclude that our results are not sensitive to the initial number of planets and the initial mass of them.

Another parameter we have varied is the initial eccentricity (and inclination) of the planetesimals without any relevant differences regarding to the previous results. We conclude that the model is robust with respect to all these assumptions.

5. Conclusions

In this paper we have studied some aspects of the oligarchic growth of planets. We have found that the presence of several planetary embryos growing simultaneously at different locations in the protoplanetary disk, generates a number of interesting features that affect the whole accretion history, specially for the innermost planets.

The results presented here clearly indicate the relevance of considering a distribution of planetesimal sizes. The density profile of the planetesimal disk is a strongly dependent function of the planetesimal size. Small planetesimal are the most affected by orbital drift and planetary accretion. This phenomenology is not possible to be adequately represented using a single-sized planetesimal population.

In any case, we judge that our calculations are still simplified in a number of aspects. Notice that we have neglected the gaseous component of the embryos that may be a substantial contribution to the total planetary mass. Thus, the dynamics of planetesimals should be deeply affected because of this portion of mass. But even more, as we neglected the gaseous envelope, we have neglected drag effects. Thus, we have grossly underestimated the effective cross section for capturing planetesimals which, in turn, is also a function of planetesimal size. Once more, we have to note the importance to consider a realistic distribution of planetesimal sizes. Nevertheless, beyond the zone inside which planets of more than 10 $M_\oplus$ can form (see Fig. 2) we expect that the description presented in this paper to be essentially correct.

Thus the results presented in this paper should be considered as a step in performing more realistic simulations of planetary formation in the oligarchic growth regime.

Acknowledgments

A.B. acknowledges ANPCyT. We acknowledge the critical reviews by Eiichiro Kokubo and John Chambers, helping us to largely improve this paper.

Appendix A. On the integration over the distribution of planetesimals

One problem we faced in allowing for a distribution of planetesimals is how to perform the integration of Eq. (25) over such a distribution.

In order to present our results in a detailed, reproducible way we shall briefly describe the employed algorithm. Notice that the distribution of planetesimal sizes is a steep function which contains most of the mass in small sized planetesimals. If we are not careful at this point we can face losses of accuracy that can spoil the whole simulation.

We found it very convenient to perform the integration $\int y\,\mathrm{d}x$ over planetesimals distribution assuming the integrand behaves as a power law $y = ax^b + c$ for three consecutive points. Because of the way we defined the planetesimal distribution we have $x_{j+1} = 2x_j$ and j runs up to 31. Then, solving for a, b, and c for the interval defined by j, $j+1$, and $j+2$, we have

$$b_j = -\frac{1}{\ln 2}\ln\left(\frac{y_j - y_{j+1}}{y_{j+1} - y_{j+1}}\right),$$

$$a_j = \frac{y_j - y_{j+1}}{x_j^b(1 - 2^{b_j})},$$

$$c_j = y_j - a_j x_j^{b_j}.$$

The integral of the function over the interval (x_j, x_{j+2}) is

$$I_j = \int_{x_j}^{x_{j+2}} y\,\mathrm{d}x = a_j \frac{4^{1+b_j}}{1+b_j} x_j^{1+b_j} + 3c_j x_j. \tag{A.1}$$

And the integral over the whole distribution I is

$$I = \sum_{j=1}^{15} I_{2j+1}. \tag{A.2}$$

If two consecutive ordinates are equal we cannot employ the power law approximation; if so we employ a Simpson rule. This did not occurred for the present set of calculations.

References

Adachi, I., Hayashi, C., Nakazawa, K., 1976. The gas drag effect on the elliptic motion of a solid body in the primordial solar nebula. Prog. Theor. Phys. 56, 1756–1771.

Benvenuto, O.G., Brunini, A., 2005. Methods for computing giant planet formation and evolution. Mon. Not. R. Astron. Soc. 356, 1383–1395.

Benz, W., Asphaug, E., 1999. Catastrophic disruptions revisited. Icarus 142, 5–20.

Bodenheimer, P., Pollack, J.B., 1986. Calculations of the accretion and evolution of giant planets: The effect of solid cores. Icarus 67, 391–408.

Brunini, A., Melita, M.D., 2002. On the accretion of Uranus and Neptune. Mon. Not. R. Astron. Soc. 330, 184–186.

Chambers, J., 2006. A semi-analytic model for oligarchic growth. Icarus 180, 496–513.

Dohnanyi, J.S., 1969. Collisional models of asteroids and their debris. J. Geophys. Res. 74, 2531–2554.

Fernández, J.A., 2005. Comets: Nature, Dynamics, Origin and Their Cosmogonical Relevance. Springer, Berlin.

Fortier, A., Benvenuto, O.G., Brunini, A., 2007. Oligarchic planetesimal accretion and giant planet formation. Astron. Astrophys. 473, 311–322.

Gear, C.W., 1971. Numerical Initial Value Problems in Ordinary Differential Equations. Prentice Hall, New York. p. 37.

Greenberg, R., 1980. Numerical simulation of planet growth: Early runaway growth. Lunar Planet. Sci. 11, 365–367.

Hasegawa, M., Nakazawa, K., 1990. Distant encounters between Keplerian particles. Astron. Astrophys. 227, 619–627.

Hayashi, C., Nakazawa, K., Nakagawa, Y., 1985. In: Black, D.C., Matthews, M.S. (Eds.), Protostars and Planets II. University of Arizona Press, Tucson, pp. 1100–1153.

Ida, S., Makino, J., 1993. Scattering of planetesimals by a protoplanet—Slowing down of runaway growth. Icarus 106, 210–227.

Inaba, S., Ikoma, M., 2003. Enhanced collisional growth of a protoplanet that has an atmosphere. Astron. Astrophys. 410, 711–723.

Inaba, S., Tanaka, H., Nakazawa, K., Wetherill, G.W., Kokubo, E., 2001. High-accuracy statistical simulation of planetary accretion: II. Comparison with N-body simulation. Icarus 149, 235–250.

Kokubo, E., Ida, S., 1998. Oligarchic growth of protoplanets. Icarus 131, 171–178.

Kokubo, E., Ida, S., 2000. Formation of protoplanets from planetesimals in the solar nebula. Icarus 143, 15–27.

Kokubo, E., Ida, S., 2002. Formation of protoplanet systems and diversity of planetary systems. Astrophys. J. 581, 666–680.

Mizuno, H., 1980. Formation of the giant planets. Prog. Theor. Phys. 64, 544–557.

Ohtsuki, K., Stewart, G.R., Ida, S., 2002. Evolution of planetesimal velocities based on three-body orbital integrations and growth of protoplanets. Icarus 155, 436–453.

Pollack, J.B., Hubickyj, O., Bodenheimer, P., Lissauer, J.J., Podolak, M., Greenzweig, Y., 1996. Formation of the giant planets by concurrent accretion of solids and gas. Icarus 124, 62–85.

Pringle, J.E., 1981. Accretion discs in astrophysics. Annu. Rev. Astron. Astrophys. 19, 137–162.

Stevenson, D.J., 1982. Formation of the giant planets. Planet. Space Sci. 30, 755–764.

Thommes, E.W., Duncan, M.J., Levison, H.F., 2003. Oligarchic growth of giant planets. Icarus 161, 431–455.

Tsiganis, K., Gomes, R., Morbidelli, A., Levison, H.F., 2005. Origin of the orbital architecture of the giant planets of the Solar System. Nature 435, 459–461.

Wetherill, G.W., Stewart, G.R., 1993. Formation of planetary embryos: Effects of fragmentation, low relative velocity, and independent variation of eccentricity and inclination. Icarus 106, 190–209.